Desalination and Water Treatment A new adsorbent (aluminum modified talc) for phosphate removal from alkaline solutions and optimization of data by central composite design

5 authors, including:

Mustafa Korkmaz
Balikesir University
21 PUBLICATIONS 343 CITATIONS

SEE PROFILE

Elif Özmetin
Balikesir University
17 PUBLICATIONS 151 CITATIONS

SEE PROFILE

Yeliz Süzen
Balikesir University
11 PUBLICATIONS 46 CITATIONS

SEE PROFILE

Elif Calgan
Balıkesir University
7 PUBLICATIONS 7 CITATIONS

SEE PROFILE

A new adsorbent (aluminum modified talc) for phosphate removal from alkaline solutions and optimization of data by central composite design

Mustafa Korkmaz*, Elif Özmetin, Yeliz Süzen, Elif Çalgan, Cengiz Özmetin

*Balıkesir University, Engineering Faculty, Environmental Engineering Department, 10145 Çağış Campus Balıkesir City Turkey,
Tel. +90 266 6121194; Fax +90 266 6121257; email: korkmazm@balikesir.edu.tr (M. Korkmaz), https://orcid.org/0000-0001-8424-6339,
email: eozmetin@balikesir.edu.tr (E. Özmetin), https://orcid.org/0000-0002-3318-4083, email: yelizyasar@balikesir.edu.tr (Y. Süzen),
https://orcid.org/0000-0003-4059-4643, email: eliftekin@balikesir.edu.tr (E. Çalgan), https://orcid.org/0000-0002-6794-1863,
email: cozmetin@balikesir.edu.tr (C. Özmetin), https://orcid.org/0000-0003-3962-9255*

ABSTRACT

A new adsorbent material, aluminum modified talc clay, was synthesized for phosphate adsorption from solutions. The raw talc and aluminum coagulation were not effective than modified talc. Due to this reason, phosphate adsorption from synthetic solutions on modified talc was investigated in a batch system as a function of pH, time, concentration, temperature, solid amount and aluminum loading effect. Optimum conditions for modified talc were determined as pH (11), temperature (40°C), concentration (200 mg/L), time (20 min), solid amount (1 g/50 mL), and aluminum loading (1.5 g AlCl₃/10 g talc/50 mL pure water). Optimization of phosphate adsorption onto modified talc was realized by central composite experimental design using Minitab 16.0 program. The statistically importance sequence of parameters were dosage, dosage–dosage, pH–dosage, pH, pH–pH, concentration, dosage–concentration, pH–concentration and concentration–concentration. The kinetics of removal obeyed the pseudo-second-order model rather than pseudo-first-order model. The isotherm data fitted well to the Langmuir isotherm. The thermodynamic analysis of phosphate adsorption indicated non-spontaneous and physical adsorption of phosphate. The rate controlling mechanism for adsorption was particle diffusion. The XRD analysis for raw talc was done. FTIR-ATR analysises for raw, modified and phosphate adsorbed modified talc were done. SEM images before and after adsorption was interpreted. According to obtained results, the modified talc was found as an effective adsorbent for phosphate removal from uncomplex wastewaters for control of eutrophication and for production of drinking water. Maximum phosphate capacity was calculated as 37.45 mg/g.

Keywords: Phosphate adsorption; Aluminum modified talc; Langmuir isotherm; Central composite design; Pseudo-second-order

1. Introduction

The eutrophication occurs due to phosphorus concentration increase in lake waters [1]. There is no gas phase of phosphorus element in the ecosystem [2]. The eutrophication is proliferation of the blue-green algae population [3]. The eutrophication prevents the usage of water in different purposes [4]. Phosphorus is generally available in waters as meta-phosphate, pyro-phosphate, ortho-phosphate, poly-phosphate and organic phosphates. The phosphate reaches into surface waters from fertilizers, decaying of forest plants, weathering of phosphate rocks, phosphate processing industries and municipal wastewaters [5]. The standart value of phosphorus (PO_4–P) is recommended as below 0.5 mg/L for drinking water consumption (Europian Council Standard) [5]. USEPA recommends to criterons for

control eutrophication: if there is discharge from point source to reservoir, total PO_4–P should be ≤0.05 mg/L), if only for reservoirs, total PO_4–P should be ≤0.025 mg/L [5]. The calcium and phosphorus play as improving role in bones [6] and high concentration of phosphate in drinking waters results in digestive system disease [5]. Phosphate removal from wastewaters and from phosphate-containing drinking water sources is therefore a global necessitate [5].

The physico-chemical techniques for phosphate removal are adsorption [1,2], ion exchange [7], coagulation [8], electro-coagulation [9], biosorption [10], biological treatment [11]. In the case of cheap adsorbents usage, adsorption is an applicable method in phosphate removal. Adsorption has been extensively investigated for phosphate removal from waters [1,2,12,13]. However, aluminum loaded talc is a new and candidate adsorbent material for phosphate adsorption from waters.

The zeta potential of clay surface controls the stability of colloids in aqueous mediums. The broken edges of clays like silicon and aluminum determine to surface potential and adsorption ability [14]. Talc framework formula is $Mg_3(Si_2O_5)_2(OH)_2$. Talc forms from two tetrahedral and one octahedral layers and it is a layered magnesium silicate [14,15]. The World talc amount has 2.4 billion ton capacity. Ultramafic talc deposits and talc deposits within dolomites are the main significant talc deposits [14,15].

Firstly, Box and Wilson defined the response surface optimization method. They determined the experimental matrix giving the maximum output with the least number of experimental runs. The model obtained from the response surface method is formed with the help of regression analysis. The importance of the main factors in the model or their interactions is determined by the regression coefficients and confidence constants (p). The response surface method is used in many areas of science and industry. In the response surface method, the effects of two or more factors on output can be determined. The results obtained can be analyzed with three-dimensional and counter graphics. The model obtained by the response surface method is wanted to estimate the optimum experimental parameter values. The effectiveness of model can be learned by the coefficient of determination value (R-adj) that should be very close to 1 [16].

In this study, phosphate adsorption was tested by raw talc, aluminum coagulation and aluminum modified talc and the effect of pH, concentration, solid amount, temperature, time and aluminum loading was investigated. Isotherm, kinetic and diffusion mechanism analysis were conducted. Optimization of phosphate adsorption data was done by central composite design tool of response surface method. XRD analysis of raw talc was done. FTIR-ATR analysis of raw talc, aluminum talc and phosphate adsorbed aluminum talc were evaluated. SEM images of modified talc and phosphate adsorbed modified talc was interpreted. The newly synthesized aluminum talc adsorbent is the promising material for adsorption and precipitation of phosphate from waters. The end product of the adsorption can be used in agriculture as phosphate and aluminum rich fertilizer. From this point of view, there would not be any adsorption worthless end waste. For instance, it was reported that the combined application by aluminum sulfate at a rate of 500 kg/hm² with organic-inorganic compound fertilizer was an effective amendment of saline-sodic soils in Songnen Plain, Northeast China [17].

2. Materials and methods

2.1. Equipments and used chemicals

The glass 100 mL sample bottles were used to fill phosphate solutions. The solutions were prepared on a magnetic stirrer (Hot Stirrer MS-300HS). The solution taking was done by automatic pipets (1, 5 mL) (Vitlab product). An incubator shaker was used for modification and phosphate adsorption experiments (JSR product). A pH meter was immersed into solutions for pH measurement and adjustment (WTW Multi 340i, Germany). A temperature controlled water circulator was connected to jacketed batch reactor for control of temperature in kinetic experiments (Labo SM 3 product). A 1.3 L jacketed batch reactor that provides to heating and cooling of water was used in kinetic experiments (İldam glass product, Turkey). A vacuum filtration device was used with special filtration tubes for separation of clay phase from liquid phase (Rocker 300 product). The prepared modified clay was dried in an oven (Nüve FN 400). KH_2PO_4 salt (136.09 g/moL) was dissolved in pure water to prepare 1,000 mg/L phosphate stock solution (PO_4^{3-}) and KOH and HCl were used for adjustment of pHs of solutions (Merck products). Phosphate analysis was done according to book of Standard Methods for Examination of Water and Wastewater by applying stannous chloride method [18]. The calibration curve for phosphate analysis was adjusted between 0 and 2 mg/L concentration. A spectrophotometer was used for measurement of phosphate absorbance values using quartz cuvettes. The percentage errors (reproducibility) for several analysis were calculated as 4.06%–16.7%. Aluminum chloride (Merck product) was used for preparation modification solutions. The raw talc clay was supplied from Emirdağ District of Afyon city in Turkey. Talc is not soluble in water, and is slightly soluble in dilute mineral acids. JCPDS card number for XRD was 83–1768. The modified talc sample with 0–850 μm particle size has 4,958.4 nm average pore diameter. XRD patter of the raw talc was analyzed to determine the framework crystallinity of clay and measure of the responsible peaks. FTIR-ATR analysis was carried out to determine the surface molecules or molecule morphology peaks.

2.2. Modification experiments

The talc clay was modified by treating 0.5, 1, 1.5, 2 g aluminum chloride amounts with different 10 g raw talc in 50 mL pure waters during 24 h at 200 rpm speed and room temperature. The modification experiments were carried out in an incubator shaker at room temperature. After treating talc, the mixture was filtered with Whatman filter paper and dried at 103°C in an oven. Optimum loading for phosphate adsorption was obtained for modification conditions of 1.5 g aluminum chloride dosage for 10 g talc in 50 mL pure water. But, further experiments were carried out with modified talc at modification conditions of 10 g aluminum chloride dosage, 100 g talc in 500 mL pure water by Jar test

apparatus. As this study aims to determine the parameters affecting phosphate adsorption by one factor at a time experiments, the application of 1.5 g aluminum chloride loading is not important. The effect of aluminum loading on phosphate adsorption was tested at experimental conditions of pH = 11, 20°C, 1,000 ppm phosphate, 50 mL phosphate solution, 200 rpm, 0–850 μm particle size, 20 min, 1 g modified talc. A 4 mL solutions were pipetted, filtered and diluted for analysis.

2.3. Time effect experiments

Time experiments were conducted in a jacketed batch reactor connected with a temperature controlled water circulator. The experimental parameters were pH = 5.6–6.24 (natural), 200 rpm, 20°C, 5 g adsorbent, 0–850 μm modified talc, 0–850 μm raw talc, 200 mg/L phosphate, 250 mL solution volume. The reason of the natural pH was to establish the optimum adsorption time and reaction degree, also there was no necessitate for application optimum pH and completing phosphate removal from synthetic solution as it was not a real wastewater. The jacketed reactor had 1.3 L volume. Time interval was 0, 5, 10, 20, 30, 40, 50 min. Firstly, 250 mL solution volume was prepared and filled to reactor and adsorbent was added while it was being stirred and heated and 4 mL solution sample was pipetted at predetermined time interval. The samples were filtered using Whatman filter paper under vacuum filtration with a special filtration tube. The filtrates were diluted and analyzed with stannous chloride method.

2.4. pH effect experiments

The pH effect was tested by adjustment of solution pHs with 0.1 M KOH and HCl solutions or concentrated HCl and KOH granules. After adjustment of pHs, concentrations and temperatures, the raw or modified talc powders with 0–850 μm particle sizes were added to the phosphate solutions. The liquid-solid mixture was treated in an incubator shaker during 20 min at 200 rpm speed, pH = 4–11, 1 g clay amount, 20°C, 50 mL, 200 mg/L, 0–850 μm particle size and at the end of adsorption period, 4 mL the solid–liquid phase was filtered with Whatman filter paper. The filtrates were diluted and analyzed. The raw talc had low performance for adsorption, therefore, only modified talc was used for further experiments. To compare the performance of alone aluminum against phosphate, aluminum coagulation with aluminum chloride was performed and for this purpose 0.1 g aluminum chloride amounts were added to the 50 mL solutions at 200 mg/L phosphate, 20°C ± 2.5°C, 100 rpm, pH = 4–11. In modification, 100 g raw talc adsorbed all aluminum cations of 10 g aluminum chloride.

2.5. Concentration effect experiments

The concentration effect of the phosphate solutions was studied by diluting 1,000 mg/L stock solution to 100–1,000 mg/L phosphate concentrations and stock solution was prepared by dissolving appropriate amount of KH_2PO_4 salt. The low concentrations were prepared by dilution and 1,000 mg/L concentrations were directly taken from stock solution. After adjustment of phosphate concentrations, the pHs and temperatures of the solutions were adjusted and 1 g modified talc was added to each of the solutions for treating in incubator shaker. These mixtures were treated during 20 min at 200 rpm speed, pH = 11, 20°C, 50 mL, 100–1,000 mg/L, 0–850 μm particle size, then 4 mL solution filtered with Whatman filter paper, diluted and analyzed.

2.6. Clay amount effect experiments

The modified talc amount effect was studied by adding 0.1, 0.25, 0.5, 1 g modified clay amounts to 50 mL solutions of which concentration, temperature and pHs were adjusted before. The clay added solutions were treated during 20 min at 200 rpm speed in an incubator shaker. At the end of the adsorption, the 4 mL solutions were filtered with Whatman filter paper, diluted and analyzed. The experimental parameters were pH = 11, 200 rpm, 20°C, 50 mL, 200 mg/L, 0–850 μm particle size, 20 min.

2.7. Temperature effect experiments

The prepared phosphate solutions were firstly adjusted to desired temperature, concentration and pHs and modified talc was added and treated in an incubator shaker during 20 min. At the end of the adsorption, the 4 mL solutions were filtered with Whatman filter paper, diluted and analyzed. The experimental parameters for phosphate adsorption were pH = 11, 200 rpm, 1,000 mg/L, 1 g modified talc, 50 mL, 0–850 μm particle size, 20 min. The temperature range was 20°C–40°C.

2.8. Optimization experiments

Optimization experiments were carried out in an orbital incubator shaker at constant experimental matrix values. The phosphate solutions adjusted at different concentrations (200–600 mg/L), pHs (3–11) and solid amounts (0.2–1 g/50 mL) were treated at temperature 20°C, 200 rpm stirring speed, 50 mL solution volume, 20 min operation time, 0–850 μm particle size. After adsorption, 4 mL treated solutions were filtered with Whatman filter paper using a special filtration tubes, diluted and phosphate analysis was done according to stannous chloride method. The reason of applying 20°C for all the solutions was for applying the room temperature because natural solution temperatures were high this value. The applying modification conditions was 1 g $Al(Cl)_3$/10 g talc/50 mL pure water instead of 1.5 g $Al(Cl)_3$/10 g talc/50 mL, because only parameters interaction effects for optimization were wanted to see.

3. Results and discussion

3.1. Modification effect on phosphate adsorption

The clay minerals are of capability for adsorption of anions and cations; however, the modification of clay minerals with proper chemicals improves the capacity when more polluted wastewaters are being treated. Nowadays, clay minerals modified with sulfactants, metal oxides or hydroxides and clay composites have been investigated by many researches [2,19–21]. In this study, the raw talc mineral

was modified with aluminum cation to enhance the capacity of talc clay because raw talc adsorbed the low amount of phosphate anion. The phosphate adsorption onto aluminum modified talc sample was studied at aluminum chloride condition of 0.5, 1, 1.5, 2 g/10 g raw talc/50 mL solution. The results are given in Fig. 1. The experimental parameters are pH (11), 20°C, 1,000 mg/L, 50 mL, 0–850 μm, 20 min, 1 g talc clay. As can be seen in Fig. 1, optimum dosage for phosphate adsorption was determined as 1.5 g aluminum chloride on 10 g of talc in 50 mL solution. The decrease of phosphate adsorption at 2 g aluminum chloride dosage was considered to be occurred due to structural deterioration of raw talc by high aluminum loading. This structural deterioration is probably due to the exchange of structural magnesium and silicon with aluminum. Adsorption capacity values for 0.5, 1, 1.5, 2 g aluminum chloride were calculated as 14.65, 16.14, 37.45 and 17.35 mg/g.

3.2. Time effect study

The time experiments of adsorption give information about the retention time for batch reactor design. The results for raw and aluminum modified talc clay are given in Fig. 2. The experimental parameters were pH = 5.60–6.24
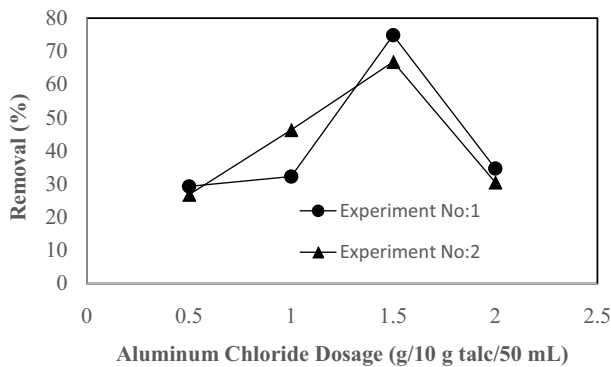

Fig. 1. Modification effect on phosphate adsorption (pH = 11, 20°C, 1,000 mg/L, 50 mL, 200 rpm, 0–850 μm, 20 min, 1 g modified talc).
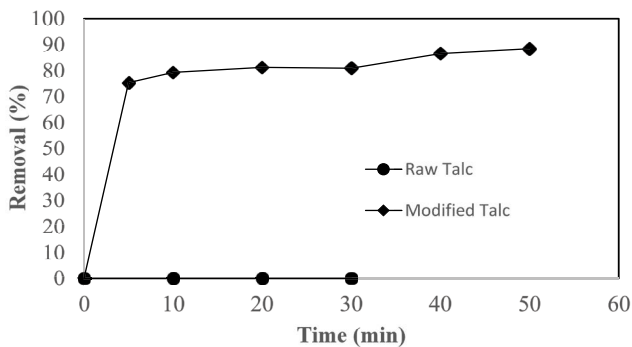

Fig. 2. Time effect on phosphate adsorption (pH (5.6–6.24 natural), 200 rpm, 20°C, 5 g adsorbent, 0–850 μm modified talc, 0–850 μm raw talc, 200 mg/L phosphate, 250 mL solution volume).

(natural), 200 rpm, 20°C, 5 g, modified talc 0–850 μm, raw talc 0–850 μm, 200 mg/L, 250 mL. The removal percentages for modified talc are 75.37%, 79.33%, 81.23%, 80.88%, 86.57%, 88.46% for 5, 10, 20, 30, 30, 40, 50 min. The capacities were 7.54, 7.93, 8.12, 8.09, 8.65, 8.85 mg/g for 5, 10, 20, 30, 40, 50 min. It is clear from the figure that raw talc did not adsorb the phosphate while modified talc shows high affinity. The adsorbed aluminum cations provided high positive charge on the raw talc and more phosphate adsorbed on it.

3.3. pH effect study

The solution pHs were adjusted in the range of 4–11 for phosphate adsorption onto raw and modified talc clay. The raw talc adsorbed low phosphate at pHs range of 8–11. The results are given in Fig. 3. The experimental parameters are 1 g clay, 20°C, 200 rpm, 50 mL, 200 mg/L, 20 min, 0–850 μm. The removal percentages for modified talc are 64.54%, 58.70%, 66.60%, 76.57%, 84.47%, 92.75% for 4, 5.5, 7, 8, 9.5, 11 pHs. The adsorption capacities were 6.45, 5.87, 6.66, 7.65, 8.45, 9.275 mg/g. Phosphate capacity of modified talc increased with pH increase from 4 to 11 and this was probably due to formation of high aluminum hydroxide on talc surface resulting adsorption and precipitation of phosphate. Further experiments were carried out by modified talc by mixture of 100 g raw talc, 10 g aluminum chloride and 500 mL pure water. The phosphate anion types based on pHs at 500 mg/L concentration and 25°C temperature are given in Fig. 4A [22] and aluminum ion types based on pHs are given in Fig. 4B [23]. As can be seen in the figures, while amorf aluminum hydroxide amounts were being increased with pH increase, the negativity of charged phosphate ions increased by increasing pHs. Thus, the phosphate adsorption onto aluminum modified talc increased by the increase of negative charged phosphates and high amorphous aluminum hydroxide and positive surface aluminum. Similarly, phosphate removal by aluminum sulphate and poly aluminum chloride showed same trend for increasing pH from 5 to 9 showing the effectiveness of Al(OH)$_3$ and Al^{3+} for phosphate removal from waters [24]. The point of zero charge values of modified talc were measured between 2–11 pHs (Fig. 5). The point of zero charge was obtained at 7.75. Due to high value of
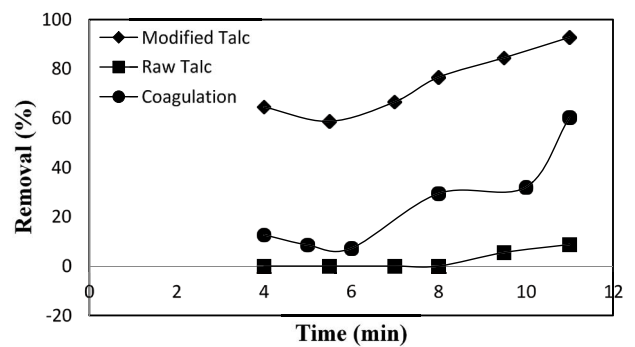

Fig. 3. pH effect on phosphate adsorption and coagulation (Adsorption: 20 min, 200 rpm, 1 g talc, 20°C, 50 mL, 200 mg/L, 0–850 μm particle size) (Coagulation: 50 mL, 100 rpm, 20°C, 0.1 g aluminum chloride, 20 min, 200 mg/L).

initial pH (11) and high concentration of potassium from KOH may cause to unchanging equilibrium pH at pH 11. The negative surface of raw talc did not adsorb the negative phosphate but aluminum hydroxide at surface of modified talc showed more affinity against the phosphate.
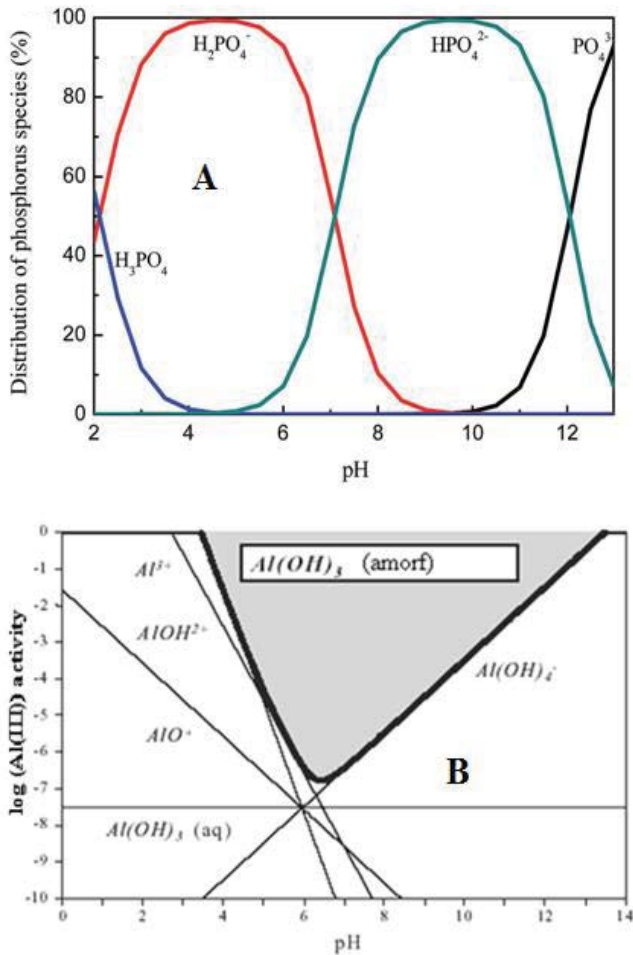

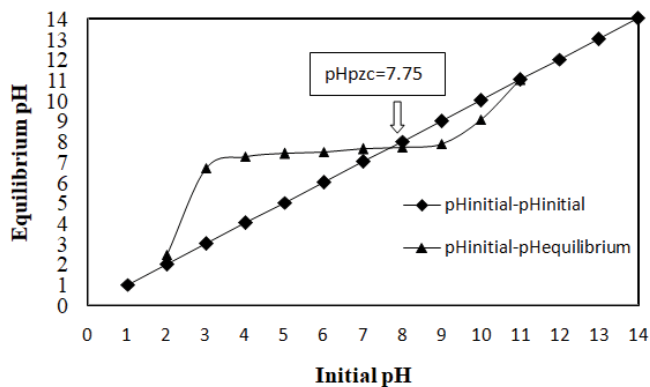Fig. 4. (A) Phosphate ion types based on pHs and (B) aluminum ion types based on pHs.

Fig. 5. Point of zero charge of modified talc (0.5 g talc, 200 rpm, 50 mL, 0–850 μm, 10 g aluminum chloride/100 g talc/500 mL, 25°C, 40 min).

The figure is given in Fig. 5. Up to pH_{pzc} value of 7.75, the modified talc surface behaved the neutralizer for hydrogen ions, above pH_{pzc}, modified talc adsorbed hydroxyl ions.

3.4. Concentration effect

Concentration effect was studied at range of 100–1,000 mg/L. The removal percentage and adsorption capacity results are given in Fig. 6. The experimental parameters are pH = 11, 200 rpm, 20°C, 50 mL, 0–850 μm, 20 min, 1 g modified clay. The removal percentages are 70.45%, 92.75%, 72.40%, 65.56%, 55.95%, 48.65%, 32.28% for 100, 200, 300, 400, 500, 750, 1,000 mg/L. Adsorption capacities were 3.52, 9.275, 10.86, 13.11, 13.99, 18.24, 16.14 mg/g for 100, 200, 300, 400, 500, 750, 1,000 mg/L. Phosphate removal efficiency of modified talc increased at low concentrations and the capacity of modified talc increased at high concentrations. This capacity increase can be related with concentration gradient increasing at high concentrations [14]. At low concentrations, the effective surface area increased the removal percentage. Similarly, boron adsorption onto aluminum modified talc showed the same trend [14]. The same concentration dependence of adsorption of Pb(II) on activated carbon was reported by Kim et al. [25]. A similar observation is noticed by other researchers for acid-factionalised biomass material for methylene blue dye removal [26]. The difference between 100 and 200 mg/L concentrations may be due to the mass balance between solid and phosphate [27].

3.5. Clay amount effect study

The modified talc clay amount effect was studied at 0.1, 0.25, 0.5, 1 g amounts and phosphate adsorption efficiency increased with increasing clay amounts. The reason of increasing efficiency of high talc amount was due to the high surface area of modified talc at high clay dosages. This is the routine trend for adsorption studies [14]. The results are given in Fig. 7. Experimental parameters are pH = 11, 200 rpm, 20°C, 50 mL, 200 mg/L, 0–850 μm, 20 min. The removal percentages are 19.88%, 39.11%, 74.51% and 92.75% for 0.1, 0.25, 0.5, 1 g dosages. Adsorption capacities are 19.88, 15.65, 14.90, 9.275 mg/g for 0.1, 0.25, 0.5, 1 g clay
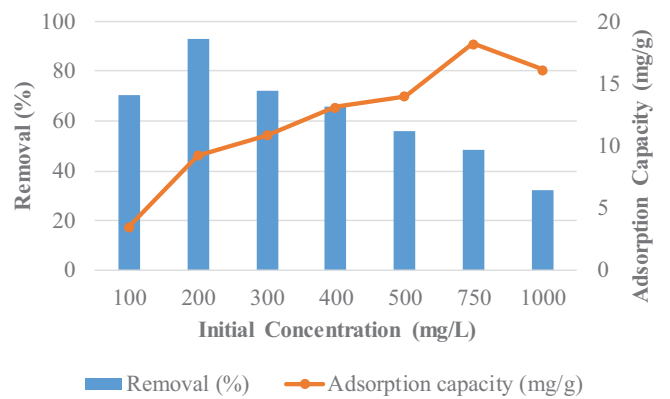

Fig. 6. Concentration effect on phosphate adsorption (20 min, 200 rpm speed, pH (11), 20°C, 50 mL, 100–1,000 mg/L, 0–850 μm particle size, 1 g modified talc).

dosages. Similar observations have been reported for Co(II) removal from waters by activated carbon and metal ion removal percentage increased with adsorbent increase [28].

3.6. Temperature effect study and thermodynamic analysis

The temperature has either endothermic or exothermic nature for adsorption of pollutants and phosphate adsorption was studied at temperature range of 20°C–40°C. The optimum temperature was determined as 40°C, and this result showed the endothermic trend of the adsorption [29,30]. The results are given in Fig. 8. Experimental parameters are pH = 11, 1,000 mg/L, 50 mL, 0–850 μm, 20 min, 1 g modified talc, 200 rpm. The thermodynamic analysis of adsorption processes can be used as tool for gaining information about nature of adsorption and spontaneity of adsorption. The Gibbs free energy, enthalpy and entropy can be calculated as follows [31].

$$\Delta G = -RT(\ln K) \tag{1}$$

$$\ln K = \frac{\Delta S}{R} - \frac{\Delta H}{RT} \tag{2}$$

$$K = \frac{Q_e}{C_e} \tag{3}$$

where ΔG is the free energy change (J/mol). ΔH is the enthalpy change (J/mol). ΔS is the entropy change (J/mol K). $K = (Q_e/C_e)$ is the equilibrium constant (L/g). T is absolute temperature (K) and R is the universal gas constant (8.314 J/mol K). Thus ΔH and ΔS can be determined from the slope and intercept of the linear Eq. (2) respectively.

The Gibbs free energy change of phosphate adsorption was calculated as 8.38, 8.2, 7.99 kJ/mol for 20°C, 30°C, 40°C. The enthalpy and entropy of adsorption were calculated as 14.17 kJ/mol and 19.7 J/mol K, respectively. The positive enthalpy and entropy indicated to endothermic adsorption and increasing adsorption–desorption rate. The figure belonging to ln(K) vs. (1/T) is given in Fig. 9. While the enthalpy range for physical adsorption is between 20 and 40 kJ/mol, this value for chemisorption is between 80 and 400 kJ/mol [32]. The positive change of Gibbs free energy with temperature indicated to the non-spontaneous nature of adsorption. The phosphate adsorption occured on surface and pore by physical binding and weakly van der Waals forces.

3.7. Kinetic study

The pseudo-first-order and pseudo-second-order kinetic models were applied to the kinetic data. Lagergren (1898) was firstly tested the pseudo-first-order rate model to oxalic acid and malonic acid binding onto charcoal and the model is as follows [33]:

$$\ln(q_e - q_t) = \ln q_e - k_1 t \tag{4}$$

In 1995, Ho described the divalent metal ions adsorption onto peat. The pseudo-second-order kinetic model is given as follows [34].

$$\frac{t}{q_t} = \left(\frac{1}{k_2 q_e^2}\right) + \left(\frac{t}{q_e}\right) \tag{5}$$

where k_1 and k_2 are pseudo-first-order and pseudo-second-order rate constants. q_e is the adsorbed amount at
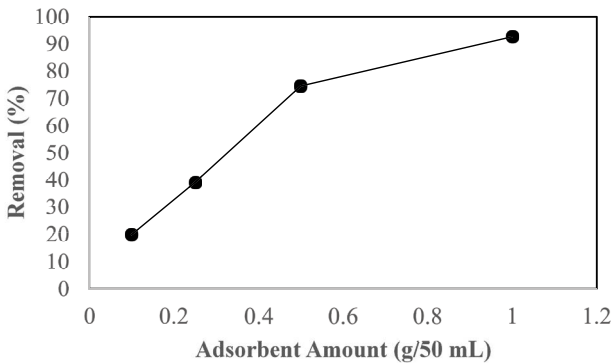
Fig. 7. Clay amount effect on phosphate adsorption (pH (11), 200 rpm, 20°C, 50 mL, 200 mg/L, 0–850 μm particle size, 20 min).
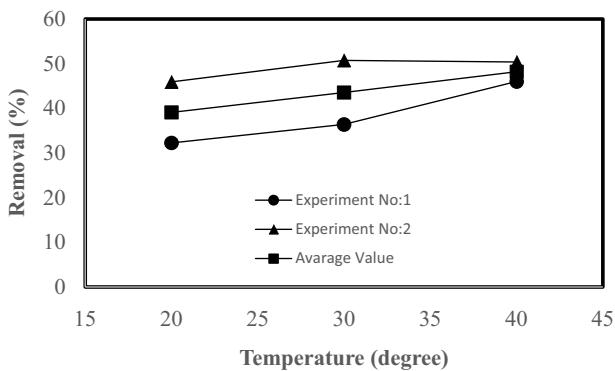
Fig. 8. Temperature effect on phosphate adsorption (pH (11), 200 rpm, 1 g modified talc, 50 mL, 1,000 mg/L, 0–850 μm particle size, 20 min).
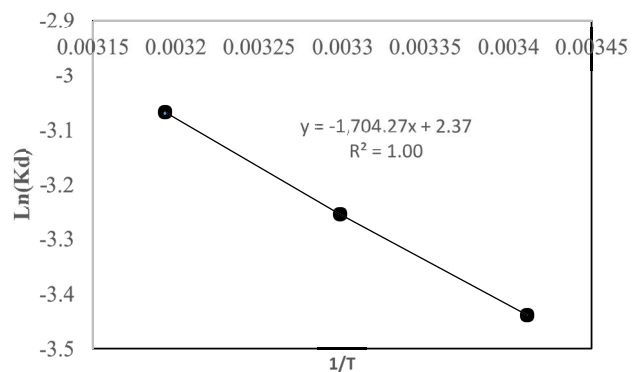
Fig. 9. Thermodynamic analysis of phosphate adsorption (the average values of temperature effect was taken).

equilibrium. q_t is the sorbed amount at any time t. The coefficient of determination values near to 1 shows the fitness of models to the data.

The kinetic data fitted to the pseudo-second-order model ($R^2 = 0.997$) rather than pseudo-first-order model ($R^2 = 0.737$). The kinetic analysis is given in Fig. 10. The mechanisms limiting the adsorption of phosphate to modified talc are surface film diffusion, particle diffusion and ash layer diffusion limitations and models are as follows [35];

A fractional approach to the equilibrium:

$$F = \left[\frac{(C_0 - C_t)}{(C_0 - C_e)} \right] \qquad (6)$$

Film-diffusion controlled process:

$$\ln(1 - F) = -k_f t \qquad (7)$$

Particle-diffusion controlled process:

$$\ln(1 - F^2) = -k_p t \qquad (8)$$

Moving boundary process (ash layer):

$$3 - 3(1 - F)^{2/3} - 2F = k_m t \qquad (9)$$

where F is the fractional approach to the equilibrium. k_f is the film diffusion rate constant. k_p is the particle diffusion rate constant. k_m is the moving boundary process (ash layer) rate constant.

According to analysis results, phosphate adsorption onto aluminum modified talc surface was firstly controlled by particle diffusion ($R^2 = 0.917$), secondly by film diffusion ($R^2 = 0.915$), third ash layer diffusion ($R^2 = 0.884$). The analysis is given in Fig. 11. As mechanism, the external aluminum cations exchanged with structural magnesium and adsorbed on external surface and pores of modified talc. Thus, the aluminum loading provided positive charge for adsorption of phosphate. The molecular size of phosphate anions is smaller than pores of modified talc. The pore size of the aluminum talc was measured as 4,958.4 nm and molecular size of phosphate molecule is about 1.15 nm. The reason of particle diffusion may be due to:

- The average pore size of modified talc is more larger than phosphate anion and its size is 4,958.4 nm but in the pores, several micrometer particles (one or two or three micrometer) can be found and also these particles have own diffuse layer (electron dust), therefore the pores may be bloked from these particle and therefore there may be pore in pore that may cause to pore diffusion.
- At high pHs, also aluminum may coagulate the small clay particles in the pores and probably bloke the pores. These situations can be seen in SEM images.

3.8. Isotherm study

The isotherm analysises give information for design of a batch reactor, adsorbent surface energy morphology and mechanism of adsorption. The most useful isotherm models are Langmuir and Freundlich models. The Langmuir isotherm is generally characterized by monolayer adsorption of pollutants and it is given as follows [36]:

$$\frac{C_e}{q_e} = \frac{1}{q_m k_L} + \frac{C_e}{q_m} \qquad (10)$$

where C_e is the equilibrium concentration in liquid phase (mg/L). q_e is the maximum amount of the phosphate adsorbed (mg/g). q_m is q_e for a complete monolayer (mg/g). k_L is a sorption equilibrium constant (L/mg).

The Freundlich isotherm generally describes the multilayer adsorption and it generally describes the physical adsorption and the model is as follows [37]:

$$\ln q_e = \ln k_F + \frac{1}{n} \ln C_e \qquad (11)$$

where C_e is the equilibrium concentration in liquid phase (mg/L). q_e is the maximum amount of phosphate adsorbed (mg/g). k_F is the Freundlich adsorption capacity. $1/n$ is sorption equilibrium constant.

The isotherm data belonging to Fig. 6 fitted to the Langmuir isotherm with a coefficient of determination value of 0.986 while Freundlich isotherm fitted with 0.871 coefficient of determination value. The isotherm parameters are given in Table 1.
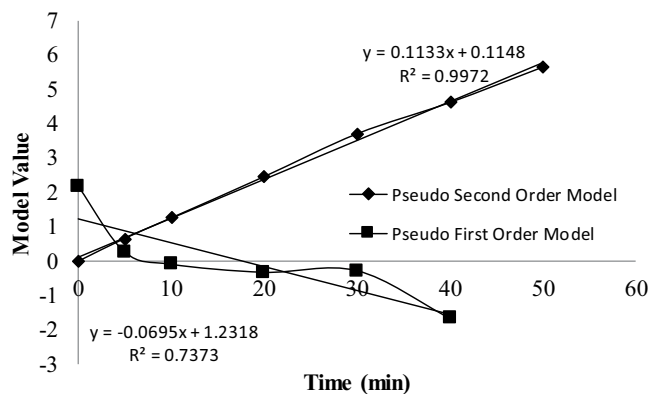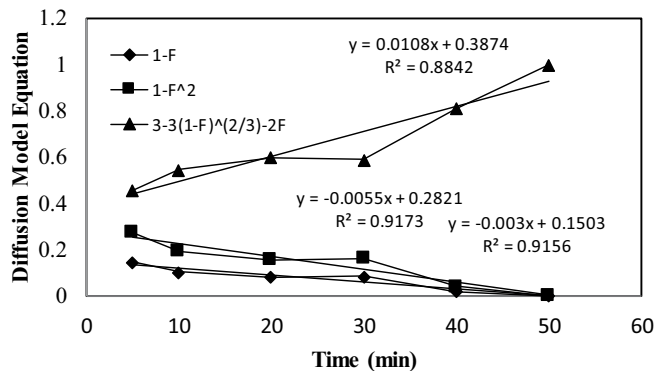

Fig. 10. Kinetic model fitness to the data.

Fig. 11. Diffusion analysis of removal.

3.9. Central composite design of experiments for phosphate adsorption

The response surface methodology was explained by Box and Wilson. They reported the very low experimental run in the experimental matrix giving the optimum output [16]. Generally, the RSM analysis is formed from three stages, namely the elimination study provides the low run, ANOVA analysis of the factors for regression model development, the analysis of factor levels to obtain the optimum conditions. The regression model is useful to relate the factor and response in a mathematical model such as the response function (Eq. 12).

$$
\begin{aligned}
\text{Removal}(\%) = b &+ b_1 X_1 + b_2 X_2 + b_3 X_3 + b_4 X_1 X_1 \\
&+ b_5 X_1 X_1 + b_5 X_2 X_2 + b_6 X_3 X_3 \\
&+ b_7 X_1 X_2 + b_8 X_1 X_3 + b_9 X_2 X_3 \\
&+ b_{10} X_1 X_2 X_3 + \varepsilon
\end{aligned}
\tag{12}
$$

The response surface optimization of pH (3–11), concentration (200–600 mg/L) and solid (0.2–1 g/50 mL) were carried out by central composite design approach using modified talc. The experimental matrix parameters are given in Table 2. The experimental matrix, responses and predicted results calculated by model are given in Table 3. The ANOVA analysis is given in Table 4. The central composite design was applied for optimization with total 15 experimental runs. For central composite design, the Minitab 16.0 program was used. The *P* values (probability constants) were used as control parameter to check the reliability of the developed statistical model, individual and interaction effects of the parameters. In general, the larger the magnitude of *t* and the smaller the value of *p*, the more significant is the corresponding coefficient term [38]. The surface plots of phosphate removal are given in Fig. 12. As can be seen in Fig. 12A, phosphate removal percentage increased with clay amount increase and concentration decrease. The removal percentage increased with concentration decrease and pH increase (Fig. 12B). Solid and pH increase raised the removal efficiency (Fig. 12C). ANOVA analysis showed that the all the factors are statistically insignificant in respect to 95% confidence level. Therefore, the regression model would be give some distortion for estimation of responses at a given experimental factors and 95% confidence level. The regression model can be given is as follows:

$$
\begin{aligned}
\text{Removal}(\%) = 50.7234 &- 6.0883\text{pH} + 16.05890 D \\
&- 0.0784C + 0.4382\text{pH} \times \text{pH} - 15.2315 D \times D \\
&+ 0.00C \times C + 7.3010\text{pH} \times D - 0.0009\text{pH} \times C \\
&- 0.0293 D \times C
\end{aligned}
\tag{13}
$$

Table 1
Isotherm analysis of data belonging to Fig. 6

Constant	Langmuir			Freundlich		
	k_L	q_m	R^2	n	k_f	R^2
Modified talc	0.0316	17.54	0.986	5.81	53.21	0.871

Table 2
The low and high values of parameters

Parameter and levels	–2	–1	0	1	2
pH	3	5	7	9	11
Solid amount (g/50 mL)	0.2	0.4	0.6	0.8	1
Concentration (mg/L)	200	300	400	500	600

Table 3
Experimental matrix for phosphate removal (20°C, 200 rpm, 50 mL, 20 min, 0–850 μm)

Parameters			Response		
pH	Solid (g/50 mL)	Concentration (mg/L)	Phosphate (%)	Capacity (mg/g)	Predicted (%)
5	0.4	300	32.8426	12.3160	21.439
9	0.4	300	49.3342	18.5003	32,227
5	0.8	300	49.7923	9.3361	31.638
9	0.8	300	63.5353	11.9129	54.107
5	0.4	500	10.2927	6.4329	2.515
9	0.4	500	11.6670	7.2919	12.583
5	0.8	500	10.4645	3.2702	10.370
9	0.8	500	37.9504	11.8595	32.119
3	0.6	400	13.4765	4.4922	14.224
11	0.6	400	49.2655	16.4218	46.761
7	0.2	400	6.6050	6.6050	6.177
7	1	400	37.2404	7.4481	35.912
7	0.6	200	26.0170	4.3362	43.937
7	0.6	600	24.9481	12.4740	3.025
7	0.6	400	20.6343	6.8781	23.481

where, pH is solution pH, C is solution concentration (mg/L), D is modified clay dosage (g/50 mL). The predicted response was recalculated by the model and compared with real data in Table 3.

3.10. XRD, SEM and FTIR-ATR analysis of adsorbents

The XRD pattern of raw talc is given in Fig. 13 showing the characteristic peaks for raw talc and some impurities.

Table 4
ANOVA analysis of phosphate removal

Term	Model constant	T	P
Constant	50.7234	0.265	0.802
pH	–6.0883	–0.273	0.796
Dosage	16.0589	0.076	0.942
Concentration	–0.0784	–0.166	0.875
pH–pH	0.4382	0.360	0.733
Dosage–Dosage	–15.2315	–0.125	0.905
Concentration–Concentration	0.0000	0.058	0.956
pH–Dosage	7.3010	0.510	0.632
pH–Concentration	–0.0009	–0.030	0.977
Dosage–Concentration	–0.0293	–0.103	0.922
P: confidence level and T: Student-t test			

JCPDS card number for XRD was 83-1768. The FTIR-ATR spectrum of raw talc, aluminum talc [14] and phosphate adsorbed modified talc sample is given in Fig. 14A–C. As can be seen in Fig. 14A and B, the bands between 3,675 and 3,660 cm^{-1} are associated with the stretching of OH associated with magnesium (Mg–OH and Mg$_3$–OH) [39,40]. Also, the peaks between 3,000 and 3,660 cm^{-1} are probably due to the aluminum hydroxide and water-OH groups (Fig. 14B) [41]. The band at 1,639 cm^{-1} is associated with the deformation vibration of water molecules (Fig. 14B). One can observe the vibration bands attributed to the Si–O–Si at 943.33, 979, 945.96 cm^{-1} [40]. The Si–O bands are seen at 755 cm^{-1} [40]. The FTIR-ATR peak increase from 3386 to 3391.87 cm^{-1} in Fig. 14C is probably due to the phosphate adsorbed on aluminum hydroxide. The peak for 1,418 cm^{-1} belongs to water molecules or organic impurity. SEM images of modified and phosphate adsorbed modified talc are given in Fig. 15. As can be seen in the figure, the more small particle are collected on phosphate adsorbed modified talc surface. Also, the pores are more clear for modified talc images. Pore blockages are more visiable for phosphate adsorbed modified talc samples.

3.11. Comparison of modified talc with other adsorbents

The modified talc clay was compared with other clays and adsorbents such as kaolinite, monmorillonite, illite, halloysite modified with different cation [42–47]. It is clear
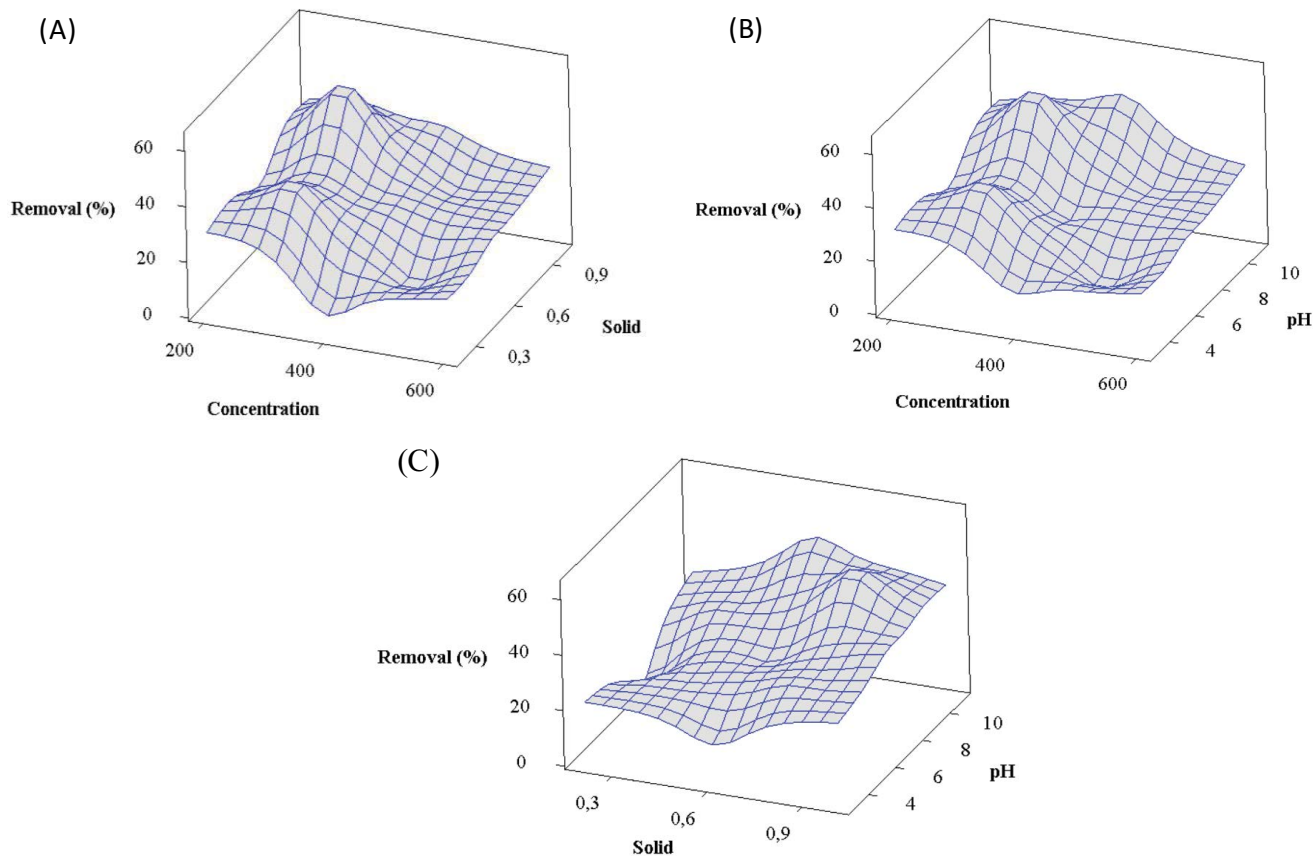

Fig. 12. Surface plots based on pHs, concentrations and modified clay amounts.
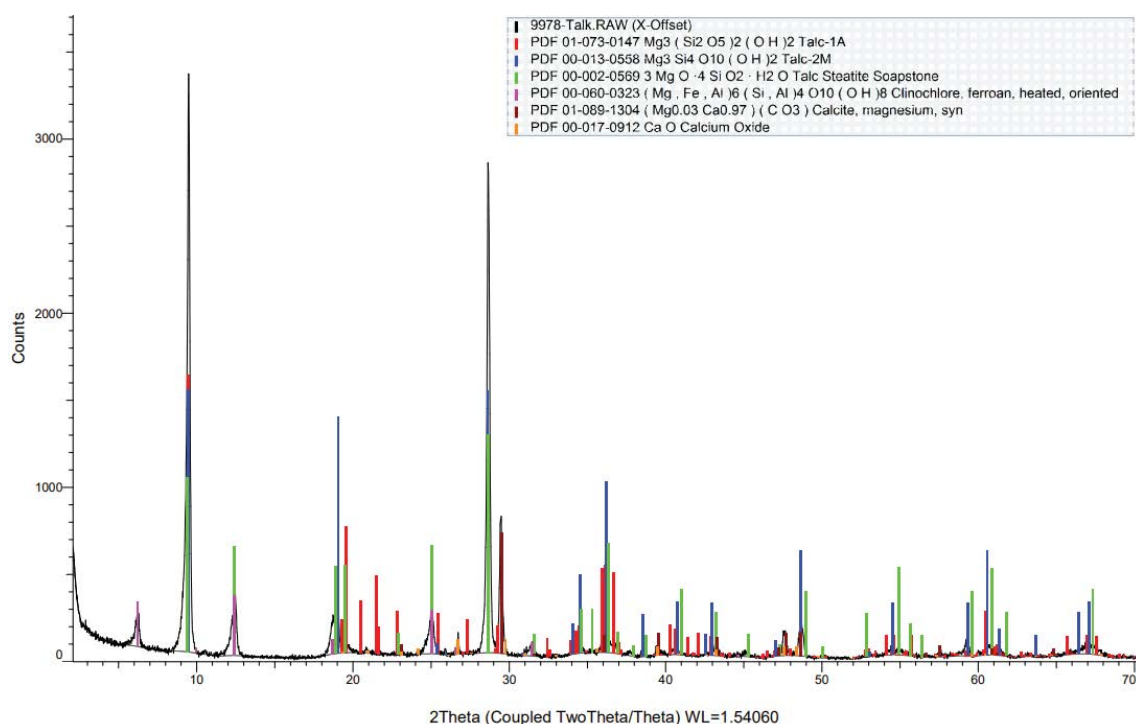
Fig. 13. XRD pattern of raw talc clay.

Table 5
Comparison of modified talc with some different modified clay adsorbents

Adsorbent	Phosphate capacity (mg/g)	Reference
Lantanium-bentonite	18	[42]
İllite saturated with different cations	0.971	[43]
Kaolinite saturated with different cations	0.516	[43]
Montmorilloinite saturated with different cations	0.638	[43]
Halloysite nanotubes	3	[44]
Iron modified halloysite nanotubes	5.5	[44]
Alginate/Goethite composite	36.4	[45]
Zirconium/magnesium-modified bentonite	13	[46]
Hydroxy-aluminum pillared bentonite	12.7	[47]
Hydroxy-iron pillared bentonite	11.2	[47]
Aluminum talc	37.45	Present Study

from Table 5 that the adsorption capacity of modified talc is very promising for phosphate removal from waters and wastewaters (Table 5). Its maximum phosphate capacity was calculated as 37.45 mg/g.

4. Conclusions

In this study, phosphate removal from synthetic solutions by raw and aluminum loaded talc clay was studied at batch system. The raw talc adsorbed low phosphate at applied conditions. The optimum parameters for modified talc were obtained as pH = 11, temperature 40°C, 1 g adsorbent, 50 mL solution volume, 200 ppm, 20 min, 1.5 g aluminum chloride for 10 g talc in 50 mL solution. The optimization of phosphate adsorption onto aluminum modified talc was done by central composite design approach testing 15 different experimental runs. Based on confidence analysis, the all factors are statistically insignificant. The process kinetic data could be described by pseudo-second-order kinetic model and particle diffusion controlled the phosphate adsorption. Langmuir isotherm fitted to the equilibrium data. It was considered that the high aluminum loading caused to structural deterioration and the removal yield lowered at 2 g aluminum chloride amount. The synthesized clay mineral was found as effective adsorbent material for phosphate removal from solutions. The coagulation of phosphate by aluminum chloride gave lower values from modified talc and it was not selected therefore.
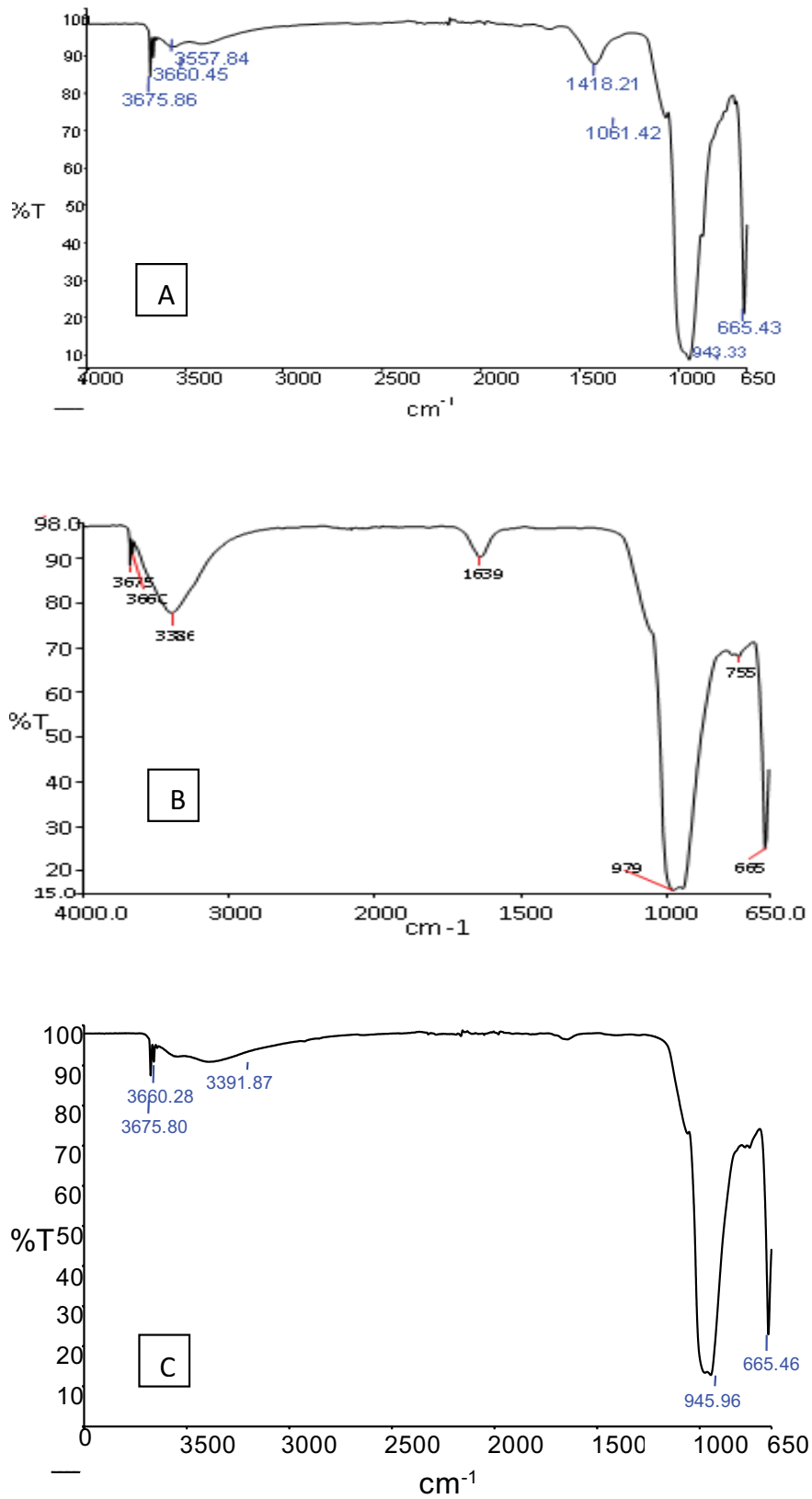
Fig. 14. The FT-IR spectrum of raw talc (A) aluminum loaded talc clay, (B) [Ref. 14] and phosphate adsorbed aluminum modified talc (C).
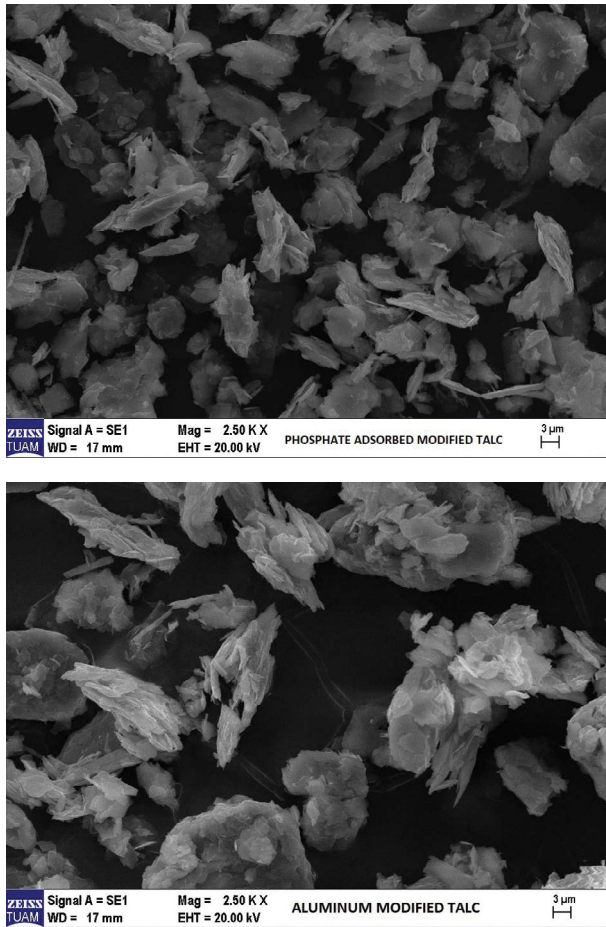
Fig. 15. SEM images of modified talc and phosphate adsorbed modified talc (200 mg/L, 250 mL, 5 g modified talc, 28.3°C, pH (5.32)).

Acknowledgement

Nomenclature

$1/n$	—	Freundlich constant
C_e	—	Concentration at equilibrium, mg/L
C_0	—	Concentration at initial, mg/L
C_t	—	Concentration at time t, mg/L
F	—	Fractional approach to the equilibrium
k_1	—	Pseudo-first-order rate constant, min⁻¹
k_2	—	Pseudo-second-order rate constant, g/mg min
k_f	—	Film diffusion rate, min⁻¹
k_F	—	Freundlich capacity
k_L	—	Langmuir constant, L/mg
k_m	—	Ash layer diffusion rate, min⁻¹
k_p	—	Particle diffusion rate, min⁻¹
K	—	Equilibrium constant, L/g
R	—	Universal gas constant, J/mol K

q_e	—	Equilibrium Capacity, mg/g
q_m	—	Maximum Capacity, mg/g
q_t	—	Capacity at time t, mg/g
t	—	Time, min
T	—	Temperature, K
ΔH	—	Enthalpy, J/mol
ΔG	—	Gibbs free energy change, J/mol
ΔS	—	Entropy change, J/mol

References

[1] T. Liu, S. Zheng, L. Yang, Magnetic zirconium-based metal–organic frameworks for selective phosphate adsorption from water, J. Colloid Interface Sci., 552 (2019) 134–141.

[2] B. Wang, W. Zhang, L. Li, W. Guo, J. Xing, H. Wang, X. Hu, W. Lyu, R. Chen, J. Song, L. Chen, Z. Hong, Novel talc encapsulated lanthanum alginate hydrogel for efficient phosphate adsorption and fixation, Chemosphere, 256 (2020) 127124, doi: 10.1016/j.chemosphere.2020.127124.

[3] K. Lu, C. Jin, S. Dong, B. Gu, S.H. Bowen, Feeding and control of blue-green algal blooms by tilapia (*Oreochromis niloticus*), Hydrobiologia, 568 (2006) 111–120.

[4] Y. Zhang, P. Luo, S. Zhao, S. Kang, P. Wang, M. Zhou, J. Lyu, Control and remediation methods for eutrophic lakes in the past 30 years, Water Sci. Technol., 81 (2020) 1099–1113.

[5] A.O. Fadiran, S.C. Dlamini, A. Mavuso, A comparative study of the phosphate levels in some surface and ground water bodies of Swaziland, Bull. Chem. Soc. Ethiop., 22 (2008) 197–206.

[6] J.P. Bonjour, Calcium and phosphate: a duet of ions playing for bone health, J. Am. Coll. Nutr., 30 (2011) 438S-48S.

[7] M. Zarrabi, M.M. Soori, M.N.S. Noori Sepehr, A. Amrane, S. Borji, H.R. Ghaffari, Removal of phosphorus by ion exchange resins: equilibrium, kinetic and thermodynamic Studies, Environ. Eng. Manage. J., 13 (2014) 891–903.

[8] M. Langer, J. Väänänen, M. Boulestreau, U. Miehe, C. Bourdon, B. Lesjean, Advanced phosphorus removal via coagulation, flocculation and microsieve filtration in tertiary treatment, Water Sci. Technol., 75 (2017) 2875–2882.

[9] K.S. Hashim, R.A. Khaddar, N. Jasim, A. Shaw, D. Phipps, P. Kot, M.O. Pedrola, A.W. Alattabi, M. Abdulredha, R. Alawsh, Electrocoagulation as a green technology for phosphate removal from river water, Sep. Purif. Technol., 8 (2019) 135–144.

[10] G. Heikal, A.E. Shahawy, Biosorption of phosphorus, total suspended and dissolved solids by dried *Phragmites australis*: isotherm, kinetic and interactive response surface methodology (IRSM) in oil and soap-derivatives industrial wastewater, Desal. Water Treat., 137 (2019) 243–259.

[11] B. Farizoglu, B. Keskinler, E. Yildiz, A. Nuhoglu, Simultaneous removal of C, N, P from cheese whey by jet loop membrane bioreactor (JLMBR), J. Hazard. Mater., 146 (2007) 399–407.

[12] Q. Zheng, L. Yang, D. Song, S. Zhang, H. Wu, S. Li, X. Wang, High adsorption capacity of Mg–Al-modified biochar for phosphate and its potential for phosphate interception in soil, Chemosphere, 259 (2020) 127469, doi: 10.1016/j.chemosphere.2020.127469.

[13] Y. Zou, R. Zhang, L. Wang, K. Xue, J. Chen, Strong adsorption of phosphate from aqueous solution by zirconium-loaded Ca-montmorillonite, Appl. Clay Sci., 192 (2020) 105638, doi: 10.1016/j.clay.2020.105638.

[14] C. Özmetin, M. Korkmaz, E. Özmetin, Y. Süzen, E. Çalgan, Boron removal from solutions by talc clay, Desal. Water Treat., 172 (2019) 260–269.

[15] B. Ersoy, S. Dikmen, A. Yıldız, R. Gören, Ö. Elitok, Mineralogical and physicochemical properties of talc from Emirdağ, Afyonkarahisar, Turkey, Turk. J. Earth. Sci., 22 (2013) 632–644.

[16] M.D. Turan, H.S. Altundoğan, Hidrometallurjik Araştırmalarda Yanıt Yüzey Yöntemlerinin (YYY) kullanımı Madencilik Cilt 50 Sayı 3 Sayfa 11–23 (2011).

[17] M. Zhou, X. Liu, Q. Meng, X. Zeng, J. Zhang, D. Li, J. Wang, W. Du, X. Ma, Additional application of aluminum sulfate with different fertilizers ameliorates saline-sodic soil of Songnen Plain in Northeast China, J. Soil Sediment, 19 (2019) 3521–3533.

[18] L.S. Clesceri, A.E. Greenberg, A.D. Eaton, Standard Methods for Examination of Water and Wastewater, 20th ed., Water Environment Federation: American Water Works Association, Washington DC, USA, 1999.

[19] L.C.A. Oliveira, R.V.R.A. Rios, J.D. Fabris, K. Sapag, V.K. Garg, R.M. Lago, Clay–iron oxide magnetic composites for the adsorption of contaminants in water, Appl. Clay Sci., 22 (2003) 169–177.

[20] F.D. Alsewailem, S.A. Aljlil, Recycled polymer/clay composites for heavy-metals adsorption, Mater. Technol., 47 (2013) 525–529.

[21] H. Xiao, B. Jie, L. Kuiran, Z. Yangguo, T. Weijun, H. Chunhui, Preparation of clay/biochar composite adsorption particle and performance for ammonia nitrogen removal from aqueous solution, J. Ocean Univ. China, 19 (2020) 729–739.

[22] M. Pan, X. Lin, J. Xie, X. Huang, Kinetic, equilibrium and thermodynamic studies for phosphate adsorption on aluminum hydroxide modified palygorskite nano-composites, RSC Adv., 7 (2017) 4492–4500.

[23] B.Z. Can, Arsenic and Boron Removal from Aqueous Solutions by Electrocoagulation Method Simultaneously and Selectively, Atatürk University Institute of Science, Ph.D. Thesis, Erzurum City, Turkey, 2010.

[24] J. Wang, J. Song, J. Lu, X. Zhao, Comparison of three aluminum coagulants for phosphorus removal, J. Water Resour. Prot., 6 (2014) 902–908.

[25] S.A. Patil, U.P. Suryawanshi, N.S. Harale, S.K. Patil, M.M. Vadiyar, M.N. Luwang, M.A. Anuse, J.H. Kim, S.S. Kolekar, Adsorption of toxic Pb(II) on activated carbon derived from agriculture waste (Mahogany fruit shell): isotherm, kinetic and thermodynamic study, Int. J. Environ. Anal. Chem., (2020) 1–17, doi: 10.1080/03067319.2020.1849648.

[26] A.H. Jawad, A.S. Abdulhameed, M.S. Mastuli, Acid-factionalized biomass material for methylene blue dye removal: a comprehensive adsorption and mechanism study, J. Taibah Univ. Sci., 14 (2020) 305–313.

[27] C. Özmetin, M. Korkmaz, Full factorial design of experiments for boron removal by iron hydroxide from colemanite mine wastewater, J. BAUN Inst. Sci. Technol., 21 (2019) 244–253.

[28] S.A. Patil, S.K. Patil, A.S. Sartape, S.C. Bhise, M.M. Vadiyar, M.A. Anuse, S.S. Kolekar, A *Pongamia pinnata* pods based activated carbon as an efficient scavenger for adsorption of toxic Co(II): kinetic and thermodynamic study, Sep. Sci. Technol., 55 (2020) 2904–2918.

[29] M. Korkmaz, C. Özmetin, B.A. Fil, E. Özmetin, Y. Yaşar, Methyl violet dye adsorption onto clinoptilolite: isotherm and kinetic study, Fresenius Environ. Bull., 22 (2013) 1524–1533.

[30] C. Özmetin, Ö. Aydın, M.M. Kocakerim, M. Korkmaz, E. Özmetin, An empirical kinetic model for calcium removal from calcium impurity-containing saturated boric acid solution by ion exchange technology using Amberlite IR–120 resin, Chem. Eng. J., 148 (2009) 420–424.

[31] B.A. Fil, C. Özmetin, M. Korkmaz, Cationic dye (methylene blue) removal from aqueous solution by montmorillonite, Bull. Korean Chem. Soc., 33 (2012) 3184–3190.

[32] G. Bayramoglu, B. Altintas, M.Y. Arica, Adsorption kinetics and thermodynamic parameters of cationic dyes from aqueous solutions by using a new strong cation-exchange resin, Chem. Eng. J., 152 (2009) 339–346.

[33] S. Lagergren, Zur theorie der sogenannten adsorption gelöster stoffe, Kungliga Svenska Vetenskapsakademiens. Handlingar, 24 (1898) 1–39.

[34] Y.S. Ho, G. McKay, Pseudo-second-order model for sorption processes, Process Biochem., 34 (1999) 451–465.

[35] F.J. Alguacil, M. Alonso, L.J. Lozano, Chromium(III) recovery from waste acid solution by ion exchange processing using Amberlite IR-120 resin: batch and continuous ion exchange modelling, Chemosphere, 57 (2004) 789–793.

[36] I. Langmuir, The constitution and fundamental properties of solids and liquids. II. Liquids, J. Am. Chem. Soc., 39 (1917) 1848–1906.

[37] H. Freundlich, Uber Die Adsorption in Losungen, Zeitschrift für physikalische, Chemie, 57 (1906) 385–470.

[38] D. Kavak, Removal of boron from aqueous solutions by batch adsorption on calcined alunite using experimental design, J. Hazard. Mater., 163 (2009) 308–314.

[39] Z. Arsoy, The influence of grinding on surface properties of talc, M.Sc. Thesis, Afyon Kocatepe University, Turkey, 2014.

[40] C.J. Ngally Sabouang, J.A. Mbey, F. Hatert, D. Njopwouo, Talc based cementitious products: effect of talc calcination, J. Asian Ceram. Soc., 3 (2015) 360–367.

[41] C.T. Johnston, S.L. Wang, S.L. Hem, Measuring the surface area of aluminum hydroxide adjuvant, J. Pharm. Sci., 91 (2002) 1702–1706.

[42] L.F.D. Castro, V.S. Brandão, L.C. Bertolino, W.F.L.D. Souzaa, V.G. Teixeira, Phosphate adsorption by montmorillonites modified with lanthanum/iron and a laboratory test using water from the Jacarepaguá Lagoon, J. Braz. Chem. Soc., 30 (2019) 641–657.

[43] A. Prssenlnes, J.W.B. Slowetrexl, D.A. Renntb, Influence of cation saturation on phosphorus adsorption by selected clay minerals, Can. J. Soil Sci., 48 (1968) 151–157.

[44] D.A. Almasri, N.B. Saleh, M.A. Atieh, G. McKay, S. Ahzi, Adsorption of phosphate on iron oxide doped halloysite nanotubes, Sci. Rep., 9 (2019) 3232.

[45] H. Siwek, A. Bartkowiak, M. Włodarczyk, Adsorption of phosphates from aqueous solutions on alginate/goethite hydrogel composite, Water, 11 (2019) 633–646.

[46] J. Lin, S. He, Y. Zhan, H. Zhang, Evaluation of phosphate adsorption on zirconium/magnesium-modified bentonite, Environ. Technol., 41 (2020) 586–602.

[47] L. Yan, Y. Xu, H. Yu, X. Xin, Q. Wei, B. Du, Adsorption of phosphate from aqueous solution by hydroxy-aluminum, hydroxy-iron and hydroxy-iron–aluminum pillared bentonites, J. Hazard. Mater., 179 (2010) 244–250.